

Strongly enhanced current densities in $\text{Sr}_{0.6}\text{K}_{0.4}\text{Fe}_2\text{As}_2+\text{Sn}$ superconducting tapes

He Lin,¹ Chao Yao,¹ Xianping Zhang,¹ Haitao Zhang,¹ Dongliang Wang,¹ Qianjun Zhang,¹ Yanwei Ma,^{1*} Satoshi Awaji,² and Kazuo Watanabe²

¹ Key Laboratory of Applied Superconductivity, Institute of Electrical Engineering, Chinese Academy of Sciences, PO Box 2703, Beijing 100190, China

² High Field Laboratory for Superconducting Materials, Institute for Materials Research, Tohoku University, Sendai 980-8577, Japan

(*) Author to whom any correspondence should be addressed. E-mail: ywma@mail.iee.ac.cn

Abstract

Improving transport current has been the primary topic for practical application of superconducting wires and tapes. However, the porous nature of powder-in-tube (PIT) processed iron-based tapes is one of the important reasons for low critical current density (J_c) values. In this work, the superconducting core density of *ex-situ* $\text{Sr}_{0.6}\text{K}_{0.4}\text{Fe}_2\text{As}_2+\text{Sn}$ tapes, prepared from optimized precursors, was significantly improved by employing a simple hot pressing as an alternative route for final sintering. The resulting samples exhibited optimal critical temperature (T_c), sharp resistive transition, small resistivity and high Vickers hardness (H_v) value. Consequently, the transport J_c reached excellent values of $5.1 \times 10^4 \text{ A/cm}^2$ in 10 T and $4.3 \times 10^4 \text{ A/cm}^2$ in 14 T at 4.2 K, respectively. Our tapes also exhibited high upper critical field H_{c2} and almost field-independent J_c . These results clearly demonstrate that PIT pnictide wire conductors are very promising for high-field magnet applications.

Since the discovery of iron-based superconductors¹, the development of wire and tape preparation for practical application was rapidly followed²⁻⁴. Particularly, 122-type iron-pnictides are most potentially useful due to their relatively high T_c up to 38 K⁵, ultrahigh H_{c2} above 100 T^{6,7} and small anisotropy γ about 1.5-2⁸. A commonly fabricating route for 122-type wires and tapes is *ex-situ* powder-in-tube (PIT) process because of its simplicity and low-cost production. However, PIT pnictide wires and tapes exhibit intrinsic weak-link behavior of grain boundaries and extrinsic factors which induce poor connection between polycrystalline grains and thus low global J_c values. Various methods including chemical addition⁹⁻¹³, rolling texture^{3, 13}, hot isostatic pressing¹⁴, cold pressing¹⁵ and cycles of cold deformation and heat treatment¹⁶ have been dedicated to improve the superconducting properties of pnictide wires and tapes. For instance, by using a texturing process plus Sn addition to improve grain connectivity, high transport J_c values were achieved in Fe-clad $\text{Sr}_{1-x}\text{K}_x\text{Fe}_2\text{As}_2$ (Sr-122) tapes¹³. High-purity and nearly 100% dense $\text{Ba}_{1-x}\text{K}_x\text{Fe}_2\text{As}_2$ (Ba-122) cores could be achieved by applying HIP technique and low-temperature sintering¹⁴. Recently, Togano *et al.* reported a large J_c enhancement by cold pressing technology, which was attributed to densification and the change of crack structure¹⁶. In past five years, the critical current densities of 122-type wires and tapes sharply increased from zero to above 10^4 A/cm² (4.2 K, 10 T), indicating its promising future for high-field applications. However, these transport J_c reported so far are still lower than the practical level, because polycrystal superconductors suffer from the disadvantages of impurity phase, inhomogeneity, low density and crack. Therefore,

further J_c enhancement of PIT tapes may be realized by optimizing precursor powders and increasing core density.

High-quality precursor powders are vital to PIT pnictide process^{14, 17-19}. Any changes in the composition or homogeneity of starting precursors could affect the superconducting performances of pnictide tapes. Our recent work already suggested that two-step sintering process of precursors helped to complete reaction and homogenous microstructure of Ag-added Sr-122 tapes whose J_c was greatly increased by an order of magnitude²⁰. On the other hand, hot pressing process could increase core density and improve grain alignment in Bi-2223 tapes, which in return led to higher zero-field $J_c(H=0)$ and in-field $J_c(H)$ ^{21, 22}. The J_c values of MgB₂ tapes were also strongly improved by hot pressing, due to much denser superconducting cores^{23, 24}. The external pressure at high temperature can reduce the tape volume and suppress the introduction of voids during the reaction process of the MgB₂ synthesis. Therefore, we expected that the porous nature of pnictide tapes, such as low density, cracks and voids, would be effectively solved by the hot pressing process.

Here we fabricated Ag-clad Sr_{1-x}K_xFe₂As₂+Sn tapes through two-step sintering process of optimized precursors (2S precursors) and hot pressing process (HP process). A high transport current to J_c (4.2 K, 10 T) $\approx 5.1 \times 10^4$ A/cm² is observed. Such a phenomenon can be qualitatively explained by the combination of improved phase formation and high core density. In addition, the conventional precursors (1S precursors) and ordinary rolled tapes (OR tapes) were also fabricated for comparison.

Results

Fig. 1 displays the magnetization versus temperature (M-T) curves of conventional 1S precursor powders and optimized 2S precursor powders. The striking result is that the diamagnetic response of 2S precursors at low temperature (below 15 K) is about two times higher than that of 1S precursors. This indicates that the second sintering process of 2S precursors with Sn addition facilitates the formation of Sr-122 superconducting phase. Nevertheless, onset T_c decreases slightly from 36.0 K for 1S precursors to 34.7 K for 2S precursors.

The X-ray diffraction (XRD) patterns of various Sr-122 tapes prepared from 1S and 2S precursors are shown in Fig. 2. All four-type samples exhibit a well ThCr_2Si_2 -type structure despite of the Ag peaks which are contributed from the Ag sheath, ensuring that a single-phase $\text{Sr}_{1-X}\text{K}_X\text{Fe}_2\text{As}_2$ superconductor is obtained in final tapes prepared from both precursors. M-T curves of these Sr-122 tapes were measured and the results are reported in Fig. 3, where all samples show a sharp transition. Compared with OR-1S and HP-1S samples, both OR-2S and HP-2S tapes produced from optimized 2S precursors exhibit an enhanced diamagnetic response at the temperature below T_c , which is consistent with the M-T observation of precursors. The onset T_c values for OR-1S, HP-1S, OR-2S and HP-2S tapes are 31.8, 32.4, 34.1 and 33.8 K, respectively. It is interesting that onset T_c is very susceptible to different precursors but hardly affected by hot pressing. Regardless of the external pressure, Onset T_c of OR-1S and HP-1S tapes are about 4 K lower than that of 1S precursors. We speculated that some non-uniform phases still remain in 1S precursors by one-step sintering process^{4, 14, 17}. In contrast, the onset T_c values of OR-2S and HP-2S tapes

display slight decrease (~0.8 K) after tape fabrication with respect to 2S precursors.

The magnetic results suggest that two-step sintering process of precursors improves the homogeneity and grain crystallization of final Sr-122 superconducting phases.

In addition, the inset of Fig. 3 shows resistivity versus temperature (R-T) curves for OR-2S and HP-2S tapes. Similar onset T_c values ~ 35.3 K are observed for both tapes. Relatively, the resistivity of OR-2S and HP-2S tapes drops to zero T_c at 34.5 and 34.7 K, respectively. The sharp resistivity transitions (< 1K) indicate well electromagnetic homogeneity of our samples^{19, 25, 26}. EDS mapping as shown in Fig. 4 further demonstrates that the elements Sr, K, Fe and As of superconducting phase homogeneously distributed throughout the superconducting core in 2S tapes (the measured stoichiometry is $\text{Sr}_{0.61}\text{K}_{0.41}\text{Fe}_2\text{As}_{2.02}$). For comparison, 1S tapes show superconducting elements enriched in some areas (supplemental Fig. S1). Obviously, the resistivity of HP-2S tape is much smaller than the value of OR-2S sample, giving strong evidence of the improvement of the grain connectivity. Magneto-resistivity curves in applied fields from 0 to 9 T of the above two samples are also measured (supplemental Fig. S2). With increasing magnetic field, the superconducting transitions of both samples shift towards lower temperature. The upper critical field H_{c2} is evaluated with the criteria of 90% of normal state resistivity respectively. The H_{c2} at zero-temperature can be deduced using the Werthamer–Helfand–Hohenberg (WHH) formula: $H_{c2}(0) = -0.693T_c(dH_{c2}/dT)$. For the OR-2S and HP-2S samples, taking $T_c = 35.3$ K, the values of $H_{c2}(0)$ are as high as 115 and 110 T.

We now turn our attention to the effects of hot pressing on final tapes. Fig. 5

shows the cross-section images of Sr-122 tapes with and without hot pressing (HP-2S and OR-2S). It is clear that hot pressing significantly reduces the tape thickness from 0.44 mm to 0.3 mm. The cross-sectional area of the superconducting core in hot-pressed tapes is 0.28 mm^2 , decreased by around 30% compared to that of the rolled tapes. Similar result was also reported in the previous PIT processed MgB_2 tapes²³. Vickers hardness (H_v) measurement was carried out for both tape samples to further investigate the change of core density. The average H_v values of the OR-2S and HP-2S tapes are 61.2 and 97.3, respectively, proving that hot pressing leads to a much denser core. However, the H_v values are still lower for Sr-122 tapes than previously reported Ba-122 tapes¹⁶, which may be caused by the different processing conditions.

Fig. 6 shows the J_c -B properties at 4.2 K of Sr-122 tapes with and without hot pressing. Only data above 2 T are given, because I_c at lower field region was too high to be measured. For the tapes without hot pressing, the J_c value of $2.0 \times 10^4 \text{ A/cm}^2$ in 10 T at 4.2 K are obtained for OR-2S tapes, which is about 34% higher than that of OR-1S tapes. The striking result of Fig. 6 is that both hot-pressed tapes (HP-1S and HP-2S) show a great enhancement of J_c values in the whole field up to 14 T. The transport J_c of HP-2S tapes reaches $5.1 \times 10^4 \text{ A/cm}^2$ in 10 T at 4.2 K. Our $\text{Sr}_{0.6}\text{K}_{0.4}\text{Fe}_2\text{As}_2+\text{Sn}$ tapes also exhibit almost field-independent J_c (H) compared to Nb_3Sn , NbTi and MgB_2 superconductors. The J_c of HP-2S samples still maintains a high value of $4.3 \times 10^4 \text{ A/cm}^2$ in 14 T, which is obviously going to be true as Sr-122 has a high upper critical field $H_{c2}(0)$ (≥ 110 T). Because of such high J_c - H performance,

it is convincible that iron-pnictide has a very promising future for practical high-field applications.

Further support to the existing J_c improvement has been obtained from the analysis of the microstructural difference between rolled and hot-pressed tapes. Figs. 7 (a-f) show typical SEM images of the superconducting core of OR-2S and HP-2S tapes. The in-plane images (a-b) and longitudinal-section images (e-f) were performed on the core surface after peeling off the Ag sheath. The samples in images (c-d) were polished carefully so that the level of porosity could be quantified. Both tape samples have well-developed grains. However, the OR-2S samples have loose microstructure with many voids and residual cracks generated during packing and cold deformation (Figs. 7 (a) and (c)), and thus the grains are not well connected. Some small crushed particles are also observed and the grain sizes vary around 2-5 μm . In contrast, as presented in Figs. 7 (b) and (d), the pores and cracks almost disappear in whole core area of HP-2S tapes, resulting in a much higher density and accordingly better connectivity between the Sr-122 grains. It should be noted that cold pressing easily introduced the crack structures which run transverse to the tape length¹⁶. However, similarly large cracks are absent in our hot-pressed samples, suggesting that hot deformation can eliminate defects effectively. The average size of plate-like grains is about 4-5 μm , which is slightly larger than that of OR-2S samples. This more uniform microstructure could further improve the grain coupling. Figs. 7(e) and (f) show the longitudinal microstructure of OR-2S and HP-2S samples, respectively. Due to the two dimensional nature of crystal structure of 122 phase⁷, most Sr-122 grains present

a planar structure in rolled tapes (Fig. 7(e)). However, some degree of grain twisting is obviously observed in hot-pressed tapes (Fig. 7(f)), which can be due to the softness of grains during hot deformation. The bending of grains could prevent the formation of cracks effectively in HP-2S samples, introducing greatly enhanced strong-links^{21, 22, 27}. Clearly, the hot pressing process in this work significantly increases the core density of pnictide tapes without crushing of grains, and thus resulting in enhanced transport properties.

On the other hand, Sr-122 grains are oriented along with the tape axis marked by white arrows in Figs. 7 (e) and (f), meaning that the grain coupling in our samples is strengthened by the simple deformation technique. This result is also confirmed by XRD analysis as shown in Fig. 2. The degree of grain alignment can be quantified by the Lotgering method as follows²⁸. The texture parameter $F = (\rho - \rho_0) / (1 - \rho_0)$, where $\rho = \sum I(00l) / I(hkl)$, $\rho_0 = \sum I_0(00l) / I_0(hkl)$. I and I_0 are the intensities of each reflection peak (hkl) for the oriented and random samples, respectively. The F values for OR-1S, OR-2S, HP-1S and HP-2S samples are 0.32, 0.35, 0.35 and 0.31, respectively. The degree of grain alignment for all samples is lower than that of Fe-clad Sr-122 tapes^{13, 15} because of using low hardness of Ag sheath. However, the F values almost remain constant after hot pressing, suggesting that the hot pressing process in this work has less effect on the degree of *c*-axis texture, because the relatively low hot pressure (~10 MPa) seems not enough to affect the grain alignments. Possibly, a further enhancement of texture may be expected with the optimization of the hot pressing conditions.

Discussion

High performance Ag-clad Sr-122 tapes have been successfully fabricated by *ex-situ* PIT method, involving the two-step intermediate sintering process of precursors and hot pressing technique. It is thought that the improved Sr-122 phase formation and high core density are responsible for the significant J_c enhancement.

Firstly, controlling the properties of precursor powders is vital to the final performance of superconductors. The precursors obtained by first conventional sintering step have large grains with few impurities¹⁷. The second annealing treatment for 2S precursors allows more Sr-122 superconducting phase to form through solid-state diffusion²⁵. Then final OR-2S and HP-2S tapes show optimal T_c , enhanced diamagnetism and sharp resistivity transition, ensuring that the improved Sr-122 phase formation has been obtained in both 2S tapes with respect to 2S precursors. Therefore, both 2S tapes exhibit better transport properties in comparison with the standard 1S tapes.

Secondly, early studies showed that the strong granularity of polycrystalline compounds could cause a strong limitation to the global current flow^{29, 30}. Indeed, the porous nature of PIT pnictide tapes has extremely negative effect on transport J_c values. By employing simple hot pressing technique as an alternative route for final sintering, we are able to obtain quite high dense superconducting core, which is a main reason for superior J_c performance as shown in Fig. 6. It is found that hot pressing is very effective to reduce the pores and cracks formed by the previous packing and cold deformation. This densification contributes to well grain

connectivity in the whole core area. On the other hand, although the superconducting cross sections of HP tapes are greatly reduced compared with those of rolled tapes, the bending of Sr-122 grains without large crack structure is observed in the hot-pressed cores, thus becoming profitable for strong-links of grains^{21, 22, 27}. This is in contrast to the result of cold-pressed tapes in which some crushed planar grains and large crack structures are easily introduced by strong cold force^{15, 16}. The HP tapes exhibit small resistivity, high H_v value and uniform microstructure. Accordingly, the remarkable J_c values of 5.1×10^4 A/cm² in 10 T and 4.3×10^4 A/cm² in 14 T at 4.2 K have been achieved in our $\text{Sr}_{0.6}\text{K}_{0.4}\text{Fe}_2\text{As}_2+\text{Sn}$ tapes. Based on the recent results, it is believed that further improvement in J_c can be expected upon optimizing process parameters.

Note added: More recently, the wire and tape preparation for iron-pnictides was rapidly developed. NIMS group reported high transport J_c in Ba-122 thin tapes by applying cold pressing process³¹. Immediately after that, our group announced that the transport J_c exceeded 10^5 A/cm² at 4.2 K and 10 T for Sr-122 tapes, which achieved the practical desired level of critical current densities³².

Methods

Sample preparation. Ag-clad $\text{Sr}_{0.6}\text{K}_{0.4}\text{Fe}_2\text{As}_2$ tapes with Sn addition were fabricated by the *ex-situ* PIT method. Sr fillings, K pieces, and Fe and As powders were used as starting materials with the nominal composition of $\text{Sr}_{0.6}\text{K}_{0.4}\text{Fe}_2\text{As}_2$. In order to compensate for the loss of elements during the sintering, the starting materials contains 25 wt% excess K and 5 wt% excess As³³. The starting materials were mixed

and ground for about 12 hours by ball-milling method, which was performed in a QM-1SP4 planetary ball mill (Nanjing NanDa Instrument Plant, China) under argon atmosphere (dry milling). The milling jars and the milling balls were made from stainless steel.

The as-milled powders were further processed to precursors and tapes. The optimized precursors (2S precursors) with Sn addition were prepared through two-step sintering process. Firstly, milled powders were heat treated at 900 °C for 35 h. The sintered bulk was ground into powders and mixed with 5 wt% Sn by hand. Secondly, these powders with Sn addition were sintered at 900 °C for 30 min again. Then the synthesized precursors were packed into Ag tubes with OD 8 mm and ID 5 mm. These tubes were sealed and then cold worked into tapes (about 0.44 mm thickness) by drawing and flat rolling. The ordinary rolled tapes (OR-2S tapes) were subsequently sintered at 850 °C for 30 min. For the hot-pressed tapes (HP-2S tapes), as-rolled tapes were sandwiched between two pieces of metal sheets and pressed at ~10 MPa at 850 °C for 30 min. Furthermore, the conventional precursors (1S precursors) were prepared by one-step sintering process (900°C/35h)^{12, 13}. The prepared precursor was added with 5 wt% Sn to improve the grain connectivity. For comparison, as-rolled and hot-pressed Sr-122 tapes (OR-1S and HP-1S tapes) were also fabricated by similar process. The detailed sample names of precursors and tapes are listed in Table I.

Measurements. Magnetization versus temperature curves were performed with a superconducting quantum interference device magnetometer (SQUID). Resistivity

measurements were carried out using a PPMS system. The cross sections were mechanical polished by emery paper and lapping paper, and then the areas of superconducting cores were calculated by optical microscope images. Vickers hardness of the tape samples was measured on the polished cross sections with 0.05 kg load and 10 s duration in a row at the center of the superconducting cross section. The phase composition and microstructure was characterized by X-ray diffraction (XRD), energy dispersive X-ray spectroscopy (EDS) and scanning electron microscope (SEM). The polished samples for SEM analysis were carried out after the mechanical polishing by emery paper and then Ar ion polishing by reactive ion etching (RIE) system. The transport current I_c at 4.2 K and its magnetic field dependence were measured by the standard four-probe method with a criterion of 1 μ V/cm at the High Field Laboratory for Superconducting Materials (HFLSM) at Sendai. Then the critical current was divided by the cross section area of the superconducting core to get the critical current density J_c . For each set of tapes, I_c measurement was performed on several samples to ensure the reproducibility.

References

1. Kamihara, Y. *et al.* Iron-based layered superconductor $\text{La}[\text{O}_{1-x}\text{F}_x]\text{FeAs}$ ($x = 0.05\text{--}0.12$) with $T_c = 26$ K. *J. Am. Chem. Soc.* **130**, 3296–3297 (2008).
2. Gao, Z. *et al.* Preparation of $\text{LaFeAsO}_{0.9}\text{F}_{0.1}$ wires by the powder-in-tube Method. *Supercond. Sci. Technol.* **21**, 105024 (2008).
3. Wang, L. *et al.* Large transport critical currents of powder-in-tube $\text{Sr}_{0.6}\text{K}_{0.4}\text{Fe}_2\text{As}_2/\text{Ag}$ superconducting wires and tapes. *Physica C*, **470**, 183 (2010).
4. Ma, Y. Progress in wire fabrication of iron-based superconductors. *Supercond. Sci. Technol.* **25**, 113001 (2012).
5. Rotter, M. *et al.* Superconductivity at 38 K in the iron arsenide $(\text{Ba}_{1-x}\text{K}_x)\text{Fe}_2\text{As}_2$. *Phys. Rev. Lett.* **101**, 107006 (2008).
6. Ni, N. *et al.* Anisotropic thermodynamic and transport properties of single-crystalline $\text{Ba}_{1-x}\text{K}_x\text{Fe}_2\text{As}_2$ ($x=0$ and 0.45). *Phys. Rev. B* **78**, 014507 (2008)
7. Wang, X. *et al.* Very strong intrinsic flux pinning and vortex avalanches in $(\text{Ba}, \text{K})\text{Fe}_2\text{As}_2$ superconducting single crystals. *Phys. Rev. B* **82**, 024525 (2010)
8. Yamamoto, A. *et al.* Small anisotropy, weak thermal fluctuations, and high field superconductivity in Co-doped iron pnictide $\text{Ba}(\text{Fe}_{1-x}\text{Co}_x)_2\text{As}_2$. *Appl. Phys. Lett.* **94**, 062511 (2009).
9. Wang, L. *et al.* The role of silver addition on the structural and superconducting properties of polycrystalline $\text{Sr}_{0.6}\text{K}_{0.4}\text{Fe}_2\text{As}_2$. *Supercond. Sci. Technol.* **23**, 025027 (2010).
10. Ding, Q. *et al.* Superconducting properties and magneto-optical imaging of $\text{Ba}_{0.6}\text{K}_{0.4}\text{Fe}_2\text{As}_2$ PIT wires with Ag addition. *Supercond. Sci. Technol.* **25**, 035019 (2012).
11. Wang, L. *et al.* Influence of Pb addition on the superconducting properties of polycrystalline $\text{Sr}_{0.6}\text{K}_{0.4}\text{Fe}_2\text{As}_2$. *Supercond. Sci. Technol.* **23**, 054010 (2010).
12. Qi, Y. *et al.* Transport critical currents in the iron pnictide superconducting wires prepared by the *ex situ* PIT method. *Supercond. Sci. Technol.* **23**, 055009 (2010).
13. Gao, Z. *et al.* High critical current density and low anisotropy in textured

$\text{Sr}_{1-x}\text{K}_x\text{Fe}_2\text{As}_2$ tapes for high field applications. *Sci. Rep.* **2**, 998 (2012).

14. Weiss, J. D. *et al.* High intergrain critical current density in fine-grain $(\text{Ba}_{0.6}\text{K}_{0.4})\text{Fe}_2\text{As}_2$ wires and bulks. *Nat. Mater.* **11**, 682 (2012).
15. Yao, C. *et al.* Microstructure and transport critical current in $\text{Sr}_{0.6}\text{K}_{0.4}\text{Fe}_2\text{As}_2$ superconducting tapes prepared by cold pressing. *Supercond. Sci. Technol.* **26**, 075003 (2013).
16. Togano, K. *et al.* Enhancement in transport critical current density of *ex situ* PIT $\text{Ag}/(\text{Ba, K})\text{Fe}_2\text{As}_2$ tapes achieved by applying a combined process of flat rolling and uniaxial pressing. *Supercond. Sci. Technol.* **26**, 115007 (2013).
17. Zhang, Z. *et al.* Effects of heating conditions on the microstructure and superconducting properties of $\text{Sr}_{0.6}\text{K}_{0.4}\text{Fe}_2\text{As}_2$. *Supercond. Sci. Technol.* **23**, 065009 (2010).
18. Togano, K. *et al.* Large transport critical current densities of Ag sheathed $(\text{Ba, K})\text{Fe}_2\text{As}_2+\text{Ag}$ Superconducting Wires Fabricated by an *ex-situ* powder-in-tube process. *Appl. Phys. Express* **4**, 043101 (2011).
19. Palenzona, A. *et al.* A new approach for improving global critical current density in $\text{Fe}(\text{Se}_{0.5}\text{Te}_{0.5})$ polycrystalline materials. *Supercond. Sci. Technol.* **25**, 115018 (2012).
20. Lin, H. *et al.* Enhanced transport critical current density in textured $\text{Sr}_{0.6}\text{K}_{0.4}\text{Fe}_2\text{As}_2 + \text{Ag}$ tapes by an intermediate sintering process of precursors. *Physica C* **490**, 37 (2013).
21. Liu, H. *et al.* Effect of hot pressing on the weak-link behaviour of Ag clad Bi based superconducting tapes. *Physica C* **259**, 187 (1996).
22. Zeng, R. *et al.* Critical current density significantly enhanced by hot pressing in Bi-2223/Ag multifilamentary tapes. *Supercond. Sci. Technol.* **11**, 1101 (1998).
23. Yamada, H. *et al.* Improvement of the critical current properties of *in situ* powder-in-tube-processed MgB_2 tapes by hot pressing. *Supercond. Sci. Technol.* **23**, 045030 (2010).
24. Wang, D. *et al.* Enhancement of J_c-B properties for binary and carbon-doped MgB_2 tapes by hot pressing. *Supercond. Sci. Technol.* **25**, 065013 (2012).

25. Lin, H. *et al.* Effects of heating condition and Sn addition on the microstructure and superconducting properties of $\text{Sr}_{0.6}\text{K}_{0.4}\text{Fe}_2\text{As}_2$ tapes. *Physica C* **495**, 48 (2013).

26. Weiss, J. D. *et al.* Mechanochemical synthesis of pnictide compounds and superconducting $\text{Ba}_{0.6}\text{K}_{0.4}\text{Fe}_2\text{As}_2$ bulks with high critical current density. *Supercond. Sci. Technol.* **26**, 074003 (2013).

27. Ma, Y. *et al.* Hot pressing behaviour of Ag-sheathed $(\text{Bi},\text{Pb})_2\text{Sr}_2\text{Ca}_2\text{Cu}_3\text{O}_x$ superconducting tapes. *Supercond. Sci. Technol.* **10**, 778 (1997).

28. Lotgering, F. Topotactical reactions with ferrimagnetic oxides having hexagonal crystal structures-I. *J. Inorg. Nucl. Chem.* **9**, 113 (1959).

29. Yamamoto, A. *et al.* Evidence for two distinct scales of current flow in polycrystalline Sm and Nd iron oxypnictides. *Supercond. Sci. Technol.* **21** 095008 (2008).

30. Putti. M. *et al.* New Fe-based superconductors: properties relevant for applications. *Supercond. Sci. Technol.* **23** 034003 (2010).

31. Gao, Z. *et al.* Achievement of practical level critical current densities in PIT $\text{Ba}_{1-x}\text{K}_x\text{Fe}_2\text{As}_2/\text{Ag}$ tapes by conventional cold mechanical deformation. *Sci. Rep.* **4** 4065 (2014).

32. Ma, Y. Advances in fabrication of iron-based superconducting wires and tapes. 26th International Symposium on Superconductivity (ISS), Tokyo, Japan, November 18–20, (2013).

33. Wang, C. *et al.* Enhanced critical current properties in $\text{Ba}_{0.6}\text{K}_{0.4+x}\text{Fe}_2\text{As}_2$ superconductor by overdoping of potassium. *Appl. Phys. Lett.* **98**, 042508 (2011).

Acknowledgments

This work is partially supported by the National '973' Program (grant No. 2011CBA00105) and the National Natural Science Foundation of China (grant Nos. 51172230, 51320105015 and 51202243).

Author contributions

Y. W. M. planned and directed the research. H. L. fabricated the tape samples and carried out resistivity, magnetization, XRD, EDS and SEM experiments. X. P. Z. and C. Y. did the high-field I_c measurement. S. A. and K. W. helped with transport measurement. D. L. W and Q. J. Z. helped with the tape preparation. X. P. Z., C.Y. and H. T. Z. contributed to manuscript preparation. H. L. and Y. W. M. wrote the manuscript. All the authors contributed to discussion on the results for the manuscript.

Additional information

Competing financial interests: The authors declare no competing financial interests.

Table I The sample names of precursors and Sr-122 tapes.

Precursors	Ordinary tapes (unpressed)	Hot pressed tapes
One-step sintered precursors (1S)	OR-1S	HP-1S
Two-step sintered precursors (2S)	OR-2S	HP-2S

Captions

Figure 1 Magnetization versus temperature curves of the conventional 1S precursor powders and the optimized 2S precursor powders.

Figure 2 XRD patterns for various Sr-122 tapes prepared from 1S and 2S precursors. The data were obtained after peeling off the Ag sheath. The peaks of $\text{Sr}_{0.6}\text{K}_{0.4}\text{Fe}_2\text{As}_2$ phase are indexed. The peaks of Ag are contributed from the Ag sheath.

Figure 3 Volumetric magnetic susceptibility as a function of temperature for various Sr122+Sn tapes with and without hot pressing. The magnetic response was evaluated by warming above T_c after zero-field-cooling to 10 K and applying a field of 20 Oe parallel to the sample's length. Inset showing the resistivity versus temperature curves of rolled OR-2S sample and hot pressed HP-2S tape. All data were obtained after peeling off the Ag sheath.

Figure 4 EDS mapping images of the superconducting core of HP-2S sample.

Figure 5 Optical microscope images of the cross sections of (a) rolled OR-2S tape and (b) hot-pressed HP-2S tape.

Figure 6 Magnetic field dependence of transport J_c at 4.2 K for various Sr-122 tapes with and without hot pressing. The applied fields up to 14 T were parallel to the tape surface.

Figure 7 SEM images showing planar views of (a) rolled OR-2S sample, (b) hot-pressed HP-2S sample, (c) polished OR-2S sample and (d) polished HP-2S sample; longitudinal sections of (e) rolled OR-2S sample and (f) hot-pressed HP-2S tape. The tape axis has been labeled using white arrows.

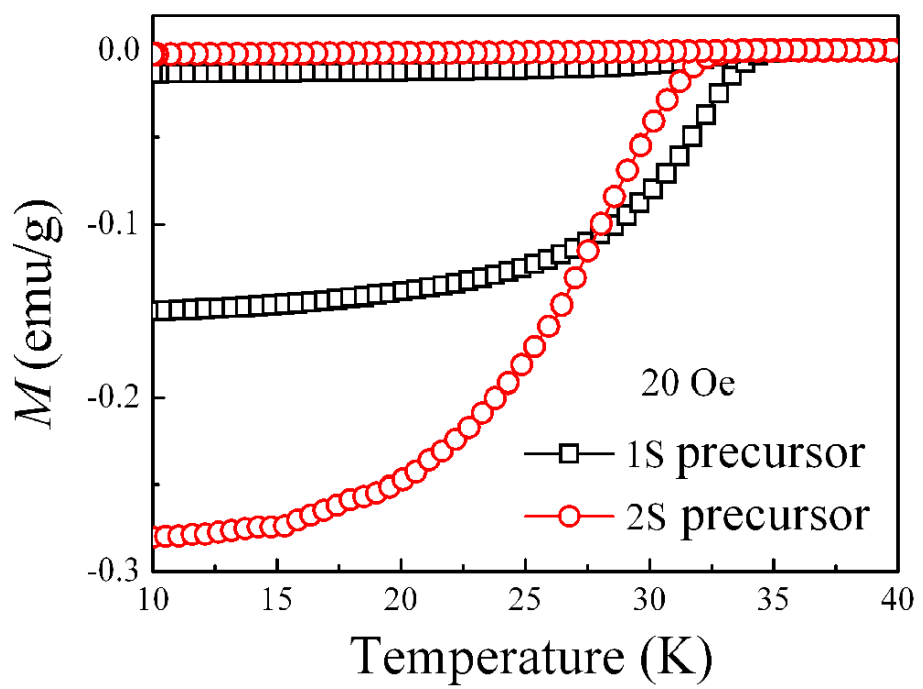


Figure 1 Lin et al.

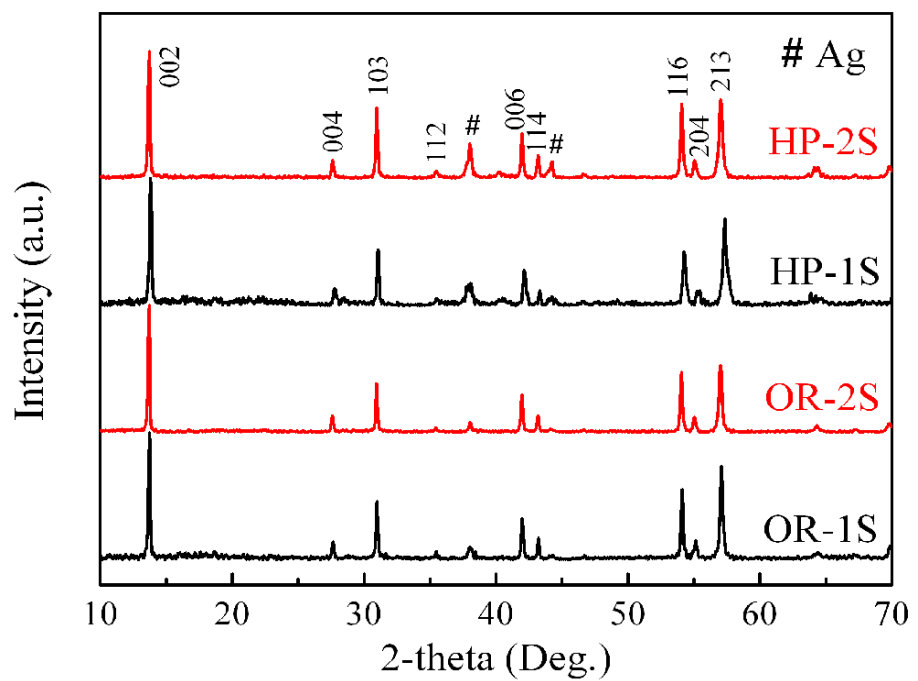


Figure 2 Lin et al.

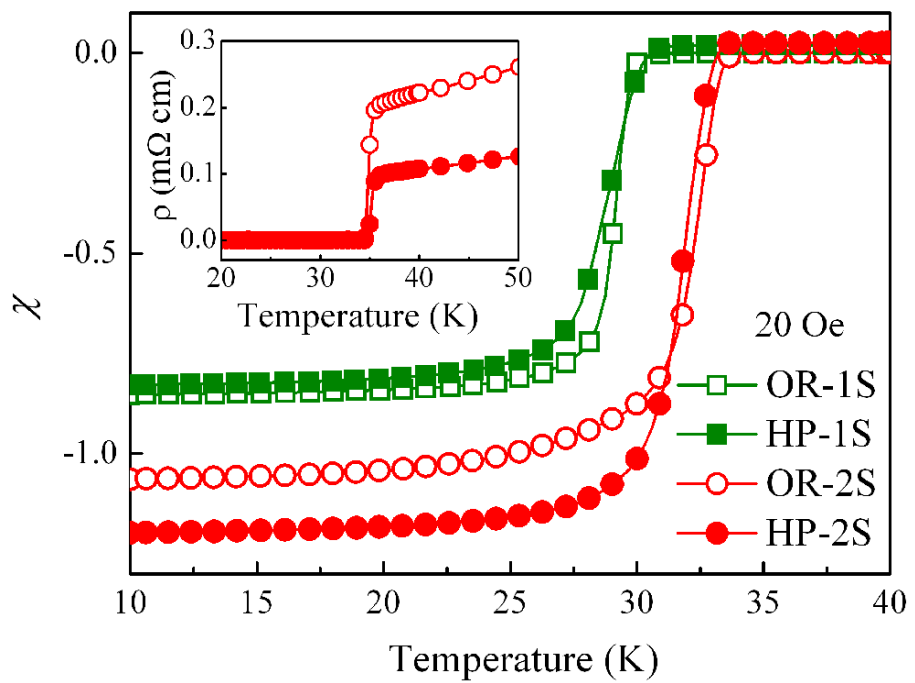


Figure 3 Lin et al.

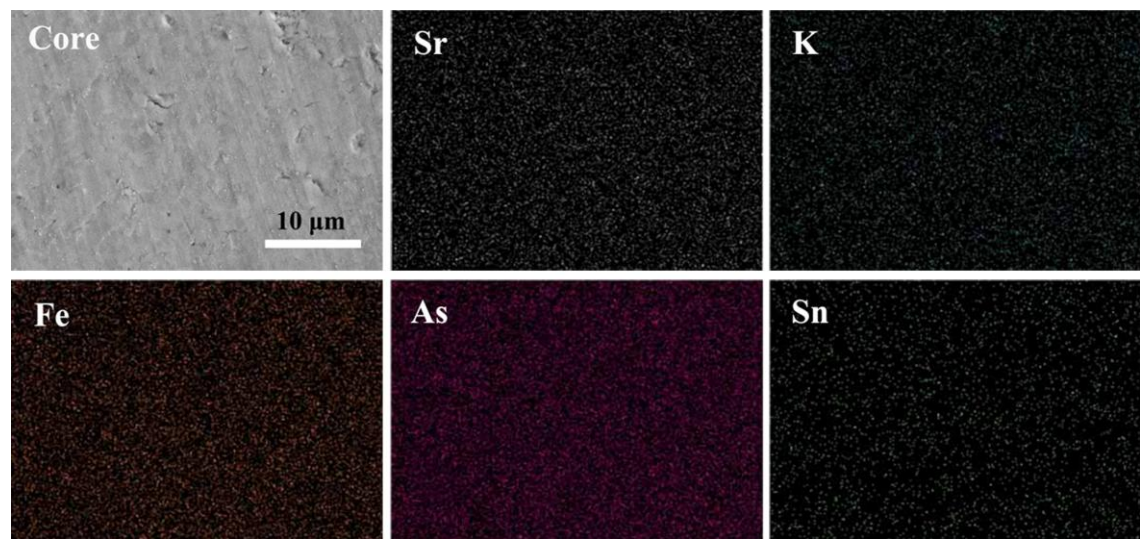


Figure 4 Lin et al.

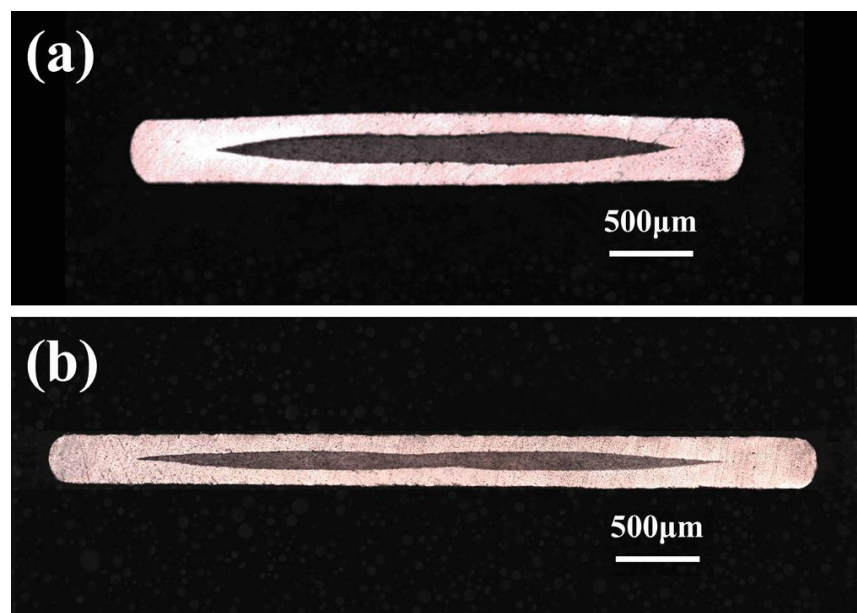


Figure 5 Lin et al.

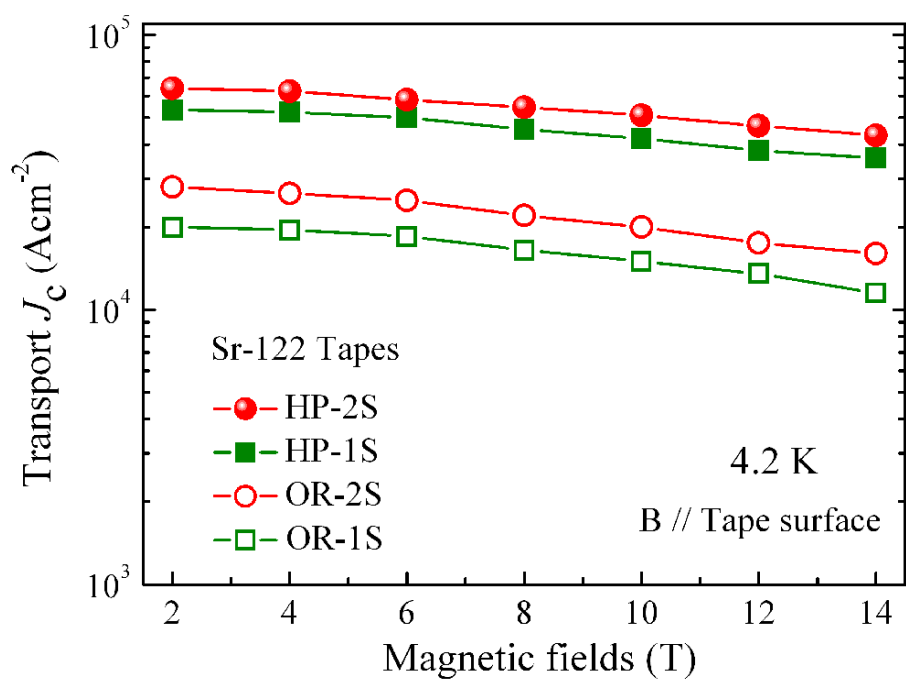


Figure 6 Lin et al.

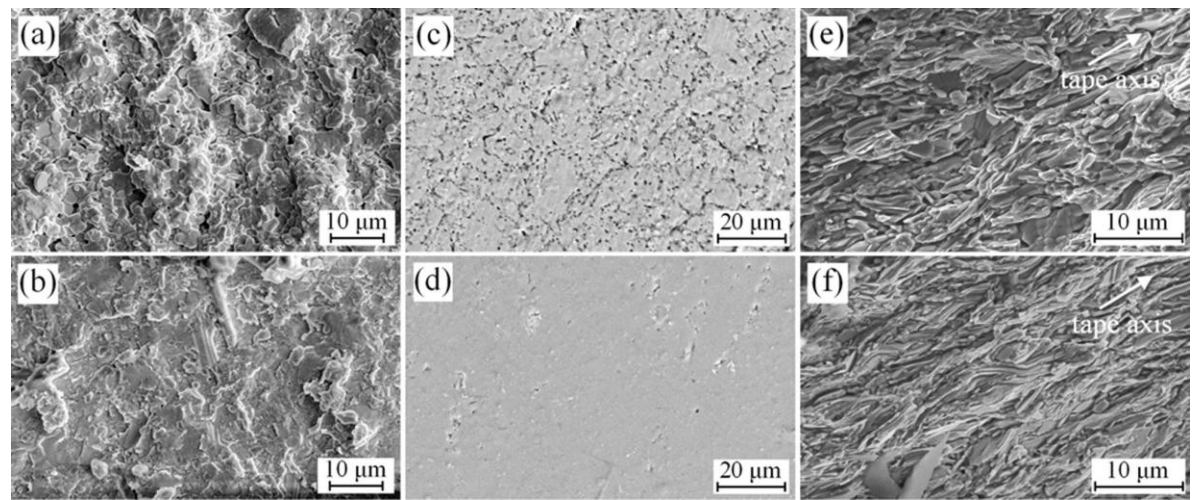


Figure 7 Lin et al.